

Chapter 3. Chaos in nonequilibrium liquid systems.

An explanation of the techniques and a review of the results in the investigation of chaos in nonequilibrium liquid systems are given. Some theoretical connections between chaoticity and fundamental issues in statistical mechanics are also discussed.

3.1 Chapter overview.

Chaos is ubiquitous: it can be found, for instance, in mathematical models that describe systems as different as rat brains and the solar system, chemical reactions and the human heart, population dynamics and stock markets. Even though an exact definition is somehow not universally established, it is commonly accepted to consider a system as chaotic when at least one of its Lyapunov exponents is positive: this denotes the presence of “sensitivity to initial conditions”, so that slight perturbations in initial values of system variables lead to unpredictable outcomes as the dynamics unfolds.

In the case of atomic systems, Lyapunov exponents measure the mean exponential rate of expansion and contraction of initially nearby phase space trajectories. For nonequilibrium steady states, not only do they provide information about the geometry and topology of the phase space, but they can also be used to extract some key quantities such as viscosity and entropy production rate. Furthermore, chaotic dynamics unveils profound connections with some of the most debated topics of statistical mechanics, such as irreversibility, the second law of thermodynamics and the derivation of macroscopic observables from microscopic properties of the system.

There have been numerous works published on chaotic systems, many of which have been developed as part of the general field of dynamical systems theory (Eckmann and Ruelle, 1985; Dorfman, 1999; Hoover, 2002; Sprott, 2003; Wiggins, 2003). Here we concentrate our attention on the techniques and results relevant to the analysis of chaotic behaviour in systems of atoms under planar shear and elongational flows, which constitute one of the central themes of this Thesis and will be discussed in great detail in the next Chapter.

The next Section is thus devoted to the explanation of the methods employed in Chapter 4 for the calculation of Lyapunov exponents, and the discussion of the so-called conjugate pairing rule, the link between exponents, thermodynamical properties and the phase space reduction in nonequilibrium many-body systems. Then, after using a one particle model, the Lorentz gas, to highlight the connections between chaos and statistical mechanics, a survey of the literature on the chaoticity of N -body nonequilibrium liquids is proposed in Section 3.3, and a presentation of recent lines of research such as Lyapunov modes and fluctuation theorems is given.

3.2 The calculation and properties of Lyapunov exponents in N -body systems.

Let us first introduce some concepts for characterizing chaoticity in atomic systems subject to steady flows, as these are the models reported in the next Chapter. Consider the equations of motion as

$$\dot{\Gamma} = \mathbf{G}(\Gamma, t) \quad (3.1)$$

where $\Gamma^T(t) \equiv (r_{1x}, r_{1y}, r_{1z}, \dots, r_{Nx}, r_{Ny}, r_{Nz}; p_{1x}, p_{1y}, p_{1z}, \dots, p_{Nx}, p_{Ny}, p_{Nz})^T$ represents a vector in the phase space for a system in 3 Cartesian dimensions and N is the number of particles. In general, systems in “ d ” dimensions can be considered, adjusting the definition of $\Gamma^T(t)$ accordingly, but we limit our analysis to $d = 3$ in the following for simplicity. We can define displacement vectors $\delta\Gamma$ between two points in the phase space, i.e. $\delta\Gamma = \Gamma_1 - \Gamma_2$. Taking the limit $\delta\Gamma \rightarrow 0$, the vectors become tangent to the phase space trajectory and obey the linearised equation

$$\delta\dot{\Gamma} = \mathbf{T} \cdot \delta\Gamma \quad (3.2)$$

where \mathbf{T} is the stability or Jacobian matrix, given by $\partial\mathbf{G}/\partial\Gamma$. The tangent vectors can be evolved forward in time via the so-called propagator $\mathbf{L}(t)$, such that

$$\delta\Gamma(t) = \mathbf{L}(t) \cdot \delta\Gamma(0) \quad (3.3)$$

Integrating Eq. (3.2) and using (3.3), we obtain the formal expression

$$\mathbf{L}(t) = \exp_L \left(\int_0^t ds \mathbf{T}(s) \right) \quad (3.4)$$

with \exp_L indicating a left-ordered exponential, where later times always appear on the left in its expansion. If we consider the matrix $(\mathbf{L}(t)^T \cdot \mathbf{L}(t))$ and its “ i th” eigenvalue ζ_i , a definition of the “ i th” Lyapunov exponent λ_i is given by (Eckmann and Ruelle, 1985)

$$\lambda_i = \lim_{t \rightarrow \infty} \frac{1}{2t} \ln \zeta_i \quad (3.5)$$

For systems out of equilibrium, the long time limit in the above equation implies that Lyapunov exponents will converge to their values only if the sample has reached a steady state. Since $(\mathbf{L}(t)^T \cdot \mathbf{L}(t))$ is usually difficult to evaluate, a more practical definition for simulations exists:

$$\lambda_i = \lim_{t \rightarrow \infty} \lim_{\delta \Gamma \rightarrow 0} \frac{1}{t} \ln \left(\frac{\|\delta \Gamma_i(t)\|}{\|\delta \Gamma_i(0)\|} \right) \quad (3.6)$$

where $\|\delta \Gamma_i(t)\|$ is the length of the orthogonal displacement vectors at time t . The equivalence between the expressions (3.5) and (3.6) at $t \rightarrow \infty$ is established through the so-called ergodic multiplicative theorem (Oseledec, 1968), which also guarantees that all the exponents are independent from the choice of initial tangent vectors in ergodic systems.

It is important to realize that any chosen $\delta \Gamma_i(0)$ will eventually align along the direction of maximum growth in the system, associated to the largest exponent λ_{\max} . In fact, imagine an initial vector $\delta \Gamma_a(0)$ and express it as a linear combination of the eigendirections of $(\mathbf{L}(t)^T \cdot \mathbf{L}(t))$, which for simplicity are supposed to be the mutually orthogonal \mathbf{u}_1 and \mathbf{u}_2 :

$$\delta \Gamma_a(0) = c_1 \mathbf{u}_1 + c_2 \mathbf{u}_2$$

If λ_1 (λ_2) is the eigenvalue associated to the direction given by \mathbf{u}_1 (\mathbf{u}_2) with $\lambda_1 > \lambda_2$, we can propagate $\delta \Gamma_a(0)$ via Eq. (3.3) and calculate its modulus to find

$$\begin{aligned} \|\delta \Gamma_a(t)\|^2 &= \|\mathbf{L}(t)(c_1 \mathbf{u}_1 + c_2 \mathbf{u}_2)\|^2 = \\ &= c_1^2 \exp(2\lambda_1 t) + c_2^2 \exp(2\lambda_2 t) \end{aligned} \quad (3.7)$$

where we implicitly used the definition of Lyapunov exponents:

$$\left[\mathbf{L}^T(t) \cdot \mathbf{L}(t) \right] \mathbf{u}_i = \exp(2\lambda_i t) \mathbf{u}_i$$

It is evident that the first exponential in (3.7) dominates over the second as $\lambda_1 > \lambda_2$, so that $\delta \Gamma_a(t)$ becomes parallel to \mathbf{u}_1 at sufficiently large times. These eigenvalues become the Lyapunov exponents defined by Eq. (3.6) in the long time limit.

This aspect is central in the design of efficient algorithms that allow the computation of all the Lyapunov exponents of the system, which in two dimensions amount to $4N$. One such procedure is represented by the method by Benettin *et al.* (Benettin *et al.*, 1976; Shimada and Nagashima, 1979; Benettin *et al.*, 1980b, 1980a), where a set of $4N$ orthonormal tangent vectors $\delta \Gamma_i^c$ is generated at $t=0$ and evolved via Eq. (3.2). Vectors are explicitly constrained to be orthogonal with the adoption of a Gram-Schmidt scheme, which is

executed at a fixed number of timesteps $n\Delta t$ ⁴, so that $\delta\Gamma_n^c \cdot \delta\Gamma_m^c = 0$ for all $m < n$. Not only does every $\delta\Gamma_i^c(t)$ rotate towards the direction of maximum growth, but its modulus quickly grows or shrinks as a consequence of the Lyapunov instability of the phase space, as Eq. (3.7) shows. Thus, vectors need also to be rescaled as time advances so that their initial length is preserved, and time averages of the logarithm of these rates of contraction or expansion give the values of the Lyapunov exponents in accordance with formula (3.6).

An equivalent algorithm which uses a different approach has been proposed by Hoover and Posch (Hoover and Posch, 1985, 1987; Hoover *et al.*, 1987). A description can also be found in (Sarman *et al.*, 1992) and the basic idea is simple: consider an initial condition $\Gamma_0(0)$ for the equations of motion (3.1) and indicate with $\Gamma_i(0)$ different small perturbations of it. Let us require that these perturbations are chosen in a way that the distances in phase space $\delta\Gamma_i^c(0) = \Gamma_i(0) - \Gamma_0(0)$ form a set of initially orthogonal tangent vectors. It is then possible to evolve the “mother” and “daughter” systems, $\Gamma_0(0)$ and $\Gamma_i(0)$ respectively, using Eq. (3.1) instead of directly propagating the tangent vectors. As time evolves, distances $\delta\Gamma_i^c(t)$ are constrained to remain constant in magnitude and mutually orthogonal through a set of $N(N+1)/2$ Lagrange multipliers ξ_{ij} :

$$\delta\dot{\Gamma}_i^c = (\dot{\Gamma}_i - \dot{\Gamma}_0) - \sum_{j=1}^{i-1} \xi_{ij} \delta\Gamma_j^c - \xi_{ii} \delta\Gamma_i^c \quad (3.8)$$

The mother-daughters distances are fixed via

$$\xi_{ii} = \frac{\delta\Gamma_i^c \cdot (\dot{\Gamma}_i - \dot{\Gamma}_0)}{(\delta\Gamma_i^c)^2}$$

and orthogonality is maintained via off diagonal elements

$$\xi_{ij} = \frac{\delta\Gamma_i^c \cdot (\dot{\Gamma}_j - \dot{\Gamma}_0) + \delta\Gamma_j^c \cdot (\dot{\Gamma}_i - \dot{\Gamma}_0)}{(\delta\Gamma_j^c)^2}$$

The Lyapunov exponents are then given by the time averages of ξ_{ii} (Hoover and Posch, 1987):

⁴ We choose $n=1$ for the simulations presented in this Thesis, but, for not excessively stiff equations of motion, the method works well for every $n \leq 10$.

$$\lambda_i = \lim_{t \rightarrow \infty} \frac{1}{t} \int_0^t \xi_{ii}(s) ds$$

We adopted the two procedures described above to code the algorithms that extract the exponents for atomic steady state systems under PSF and PEF, in the thermodynamic ensembles we discussed in Subsection 1.3.6. As said, we use a Gaussian mechanism for the NVT and NVE regimes and a Nosé-Hoover barostat in conjunction with a Gaussian isokinetic thermostat for NpT constrained dynamics. We validated the programmes against available data in the literature for PSF particle systems (see next Section), checking that results from the two methods are in agreement with each other within statistical uncertainty. To avoid redundancy, the analysis in Chapter 4 will be carried out only with the use of data obtained by the method by Benettin *et al.*

A very important property that reflects the symmetry of the Lyapunov spectrum of a dynamical system is the so-called conjugate-pairing rule, and its relevance for the calculation of transport coefficients will be explained shortly. As said, given N degrees of freedom in a d dimensional model which are unrelated to the conserved quantities in the sample, there will be $2dN$ non-trivial exponents. CPR states that, in the limit as $t \rightarrow \infty$, for every exponent λ_i there exist a conjugate $\lambda_{i'}$ such that $\lambda_i + \lambda_{i'} = \chi$, where χ is constant for every i, i' . This is equivalent to say that if we order the exponents according to their value and form pairs coupling the highest with the lowest, the second highest with the second lowest and so on, CPR is satisfied when each sum of pairs has the same value. An immediate consequence is that only half of the spectrum needs to be evaluated for systems that comply with conjugate pairing. Using Eq. (3.5), it can be shown (for a discussion see (Searles *et al.*, 1998)) that this happens if and only if the eigenvalues ζ_i of $(\mathbf{L}(t)^T \cdot \mathbf{L}(t))$ are paired in the infinite time limit, so that for every ζ_i there is a conjugate $\zeta_{i'} = \exp(2\chi t)/\zeta_i$. This in turn allows proof that CPR holds if there exists a matrix \mathbf{K} which satisfies the following relation in the limit as $t \rightarrow \infty$:

$$(\mathbf{L}(t)^T \cdot \mathbf{L}(t)) \cdot \mathbf{K} \cdot (\mathbf{L}(t)^T \cdot \mathbf{L}(t)) = \exp(2\chi t) \mathbf{K} \quad (3.9)$$

This *necessary* condition is rather hard to use for the models we are interested in, due to the definition (3.4) of the propagator $\mathbf{L}(t)$. On the other hand, a more convenient *sufficient* condition can be considered: assuming that a time-independent matrix \mathbf{K} with the

properties

$$\begin{aligned}\mathbf{T}' \cdot \mathbf{K} + \mathbf{K} \cdot \mathbf{T} &= \chi \mathbf{K} \\ \mathbf{K}' \cdot \mathbf{K} &= k \mathbf{1}\end{aligned}\tag{3.10}$$

can be found, it is possible to demonstrate (Abraham and Marsden, 1987) that Eq. (3.9) is satisfied and CPR applies. Eq. (3.10) involves the calculation of the stability matrix only, and can be conveniently used to prove that a system obeys conjugate pairing, but not that it violates it.

As an example, let us consider the SLLOD equations of motions for adiabatic PSF and PEF systems, respectively given by expressions (1.20) and (1.26). The latter are symplectic and the Jacobian is given by

$$\mathbf{T}_0^{PEF} = \begin{pmatrix} \mathbf{A} & \mathbf{1} \\ \frac{\partial \mathbf{F}}{\partial \mathbf{r}} & -\mathbf{A} \end{pmatrix}\tag{3.11}$$

where $\frac{\partial \mathbf{F}}{\partial \mathbf{r}}$ indicates the block given by the force derivatives with respect to particle positions, $\mathbf{1}$ is the unit block and \mathbf{A} represents the $3N \times 3N$ dimensional block

$$\mathbf{A} = \begin{pmatrix} \dot{\varepsilon} & 0 & 0 & & & \\ 0 & -\dot{\varepsilon} & 0 & & & \mathbf{0} \\ 0 & 0 & 0 & & & \\ & & & \ddots & & \\ & & & & \dot{\varepsilon} & 0 & 0 \\ \mathbf{0} & & & & 0 & -\dot{\varepsilon} & 0 \\ & & & & 0 & 0 & 0 \end{pmatrix}$$

with $\dot{\varepsilon}$ being the elongational rate. If the matrix \mathbf{K} is chosen to be the usual symplectic \mathbf{J}

$$\mathbf{J} = \begin{pmatrix} \mathbf{0} & \mathbf{1} \\ -\mathbf{1} & \mathbf{0} \end{pmatrix}$$

it is easy to verify that Eqs. (3.10) are satisfied with $\chi=0$, and this is true for every Hamiltonian system whenever the condition $\mathbf{K} = \mathbf{J}$ is imposed (Dragt, 1978). For the case of SLLOD PSF, an expression similar to (3.11) can be obtained:

$$\mathbf{T}_0^{PSF} = \begin{pmatrix} \mathbf{B} & \mathbf{1} \\ \frac{\partial \mathbf{F}}{\partial \mathbf{r}} & -\mathbf{B} \end{pmatrix}\tag{3.12}$$

but the subunits in the $3N \times 3N$ block \mathbf{B} are instead given by

$$\mathbf{b} = \begin{pmatrix} 0 & \dot{\gamma} & 0 \\ 0 & 0 & 0 \\ 0 & 0 & 0 \end{pmatrix}$$

making it impossible to find a \mathbf{K} for which the sufficient condition (3.10) is satisfied. For instance, if for adiabatic SLLOD PSF we try $\mathbf{K} = \mathbf{J}$ as in PEF, the first of Eqs. (3.10) reduces to $\mathbf{T}^t \cdot \mathbf{J} + \mathbf{J} \cdot \mathbf{T} = \mathbf{C}$, with

$$\mathbf{C} = \begin{pmatrix} \mathbf{0} & \mathbf{B}^t - \mathbf{B} \\ \mathbf{B}^t - \mathbf{B} & \mathbf{0} \end{pmatrix}$$

not being null because $\mathbf{B}^t \neq \mathbf{B}$.

Eq. (3.10) can be also used to verify that CPR holds when Hamiltonian systems are coupled to a constant Gaussian multiplier, which represents a particular example of a class of so-called μ -symplectic systems, for which conjugate pairing is satisfied with $\chi = \mu = \text{const}$. Consider SLLOD PEF and imagine that the isokinetic constraint in Eqs. (1.35) is substituted by a constant value α_0 . Expression (3.11) changes to

$$\mathbf{T}_{\alpha_0}^{PEF} = \begin{pmatrix} \mathbf{A} & \mathbf{1} \\ \frac{\partial \mathbf{F}}{\partial \mathbf{r}} & -\alpha_0 \mathbf{1} - \mathbf{A} \end{pmatrix} \quad (3.13)$$

and we can use the result for the adiabatic case to see that

$$\begin{aligned} \left(\mathbf{T}_{\alpha_0}^{PEF} \right)^T \cdot \mathbf{J} + \mathbf{J} \cdot \mathbf{T}_{\alpha_0}^{PEF} &= \left(\mathbf{T}_0^{PEF} + \begin{pmatrix} \mathbf{0} & \mathbf{0} \\ \mathbf{0} & -\alpha_0 \mathbf{1} \end{pmatrix} \right)^T \cdot \mathbf{J} + \mathbf{J} \cdot \left(\mathbf{T}_0^{PEF} + \begin{pmatrix} \mathbf{0} & \mathbf{0} \\ \mathbf{0} & -\alpha_0 \mathbf{1} \end{pmatrix} \right) = \\ &= \begin{pmatrix} \mathbf{0} & \mathbf{0} \\ \mathbf{0} & -\alpha_0 \mathbf{1} \end{pmatrix} \begin{pmatrix} \mathbf{0} & \mathbf{1} \\ -\mathbf{1} & \mathbf{0} \end{pmatrix} + \begin{pmatrix} \mathbf{0} & \mathbf{1} \\ -\mathbf{1} & \mathbf{0} \end{pmatrix} \begin{pmatrix} \mathbf{0} & \mathbf{0} \\ \mathbf{0} & -\alpha_0 \mathbf{1} \end{pmatrix} = \\ &= -\alpha_0 \begin{pmatrix} \mathbf{0} & \mathbf{1} \\ -\mathbf{1} & \mathbf{0} \end{pmatrix} = -\alpha_0 \mathbf{J} \end{aligned}$$

meaning that the pairing occurs with $\chi = -\alpha_0$. We will verify numerically in Subsection 4.2.4 that this result holds for elongation, whereas an equivalent SLLOD PSF system presents divergences which clearly point at a violation of CPR.

It has also been proven that a conservative autonomous system coupled to a Gaussian

mechanism is μ -symplectic (Dettmann and Morriss, 1996b; Morriss and Dettmann, 1998): if a reduced phase space is considered, where tangent vectors that alter the conserved energy and are along the direction of the flow are excluded, χ is equal to $-\langle\alpha\rangle$, where brackets indicate a time average. PSF and PEF systems we will consider in Chapter 4 are neither autonomous nor μ -symplectic, and numerical data will show that CPR is satisfied for the latter with $\chi \neq -\langle\alpha\rangle$, when small size dependent corrections are taken into account. In that case, the stability matrix can be expressed as

$$\mathbf{T}_\alpha^{PEF} = \begin{pmatrix} \mathbf{A} & \mathbf{1} \\ \frac{\partial \mathbf{F}}{\partial \mathbf{r}} & -\alpha \mathbf{1} - \mathbf{A} \end{pmatrix} + \begin{pmatrix} \mathbf{0} & \mathbf{0} \\ -\frac{\partial \alpha}{\partial \mathbf{r}} \mathbf{p} & -\frac{\partial \alpha}{\partial \mathbf{p}} \mathbf{r} \end{pmatrix} \quad (3.14)$$

and the second term is responsible for $O(1/N)$ fluctuations in the sum of Lyapunov pairs.

There are other two important aspects relative to Lyapunov exponents to discuss, namely their role in determining the phase space contraction and the transport coefficient associated with nonequilibrium steady states.

Using a terminology that will be clear shortly (Cohen, 1994), the phase space contraction factor $\Lambda(\Gamma)$ is defined as

$$\Lambda(\Gamma) = \frac{\partial}{\partial \Gamma} \cdot \dot{\Gamma} \quad (3.15)$$

This term also appears in the well-known Liouville equation (Goldstein, 1980), which describes the evolution of the density function $f(\Gamma, t)$:

$$\frac{df(\Gamma, t)}{dt} = \frac{\partial f(\Gamma, t)}{\partial t} + \dot{\Gamma} \cdot \frac{\partial f(\Gamma, t)}{\partial \Gamma} = -f(\Gamma, t) \frac{\partial}{\partial \Gamma} \cdot \dot{\Gamma} \quad (3.16)$$

Eq. (3.16) is valid for all phase points, i.e. including those from $\Gamma(0)$ to $\Gamma(t)$, and its integration gives

$$f(\Gamma(t), t) = \exp \left[- \int_0^t \Lambda(\Gamma(s)) ds \right] f(\Gamma(0), 0) \quad (3.17)$$

which has been referred to as the Lagrangian form of the Kawasaki distribution function (Evans and Searles, 2002). The last two formulae can be related if we remember that $f(\Gamma, t)$ is, by definition, the ratio between the number of ensemble points δM and the

volume element $\delta\hat{V}(\Gamma(t))$, i.e. $f(\Gamma,t) = \delta M / \delta\hat{V}(\Gamma(t))$. Consider now a volume element that moves along a phase space trajectory and contains a constant set of points: by definition δM does not change and Eq. (3.17) implies

$$\delta\hat{V}(\Gamma(t)) = \exp\left[\int_0^t \Lambda(\Gamma(s)) ds\right] \delta\hat{V}(\Gamma(0)) \quad (3.18)$$

As discussed in Section 3.2, the sum of the $6N$ Lyapunov exponents is obtained from the limiting expression (3.6), which implies the following relation between the volume element spanned by $6N$ mutually orthogonal vectors and the sum of exponents

$$\sum_{i=1}^{6N} \lambda_i = \lim_{t \rightarrow \infty} \lim_{\delta\hat{V} \rightarrow 0} \frac{1}{t} \ln \frac{\delta\hat{V}(\Gamma(t))}{\delta\hat{V}(\Gamma(0))} \quad (3.19)$$

Then, combining Eqs. (3.18) and (3.19) gives

$$\sum_{i=1}^{6N} \lambda_i = \lim_{t \rightarrow \infty} \frac{1}{t} \int_0^t \Lambda(\Gamma(s)) ds = \langle \Lambda(\Gamma) \rangle \quad (3.20)$$

where the final equality has been obtained using the assumption of ergodicity. For a Hamiltonian system at equilibrium, $\Lambda(\Gamma)$ vanishes by virtue of symplecticity, the phase-space is conserved as stated by Liouville's theorem and the sum of exponents is zero, in line with our previous considerations about conjugate pairing.

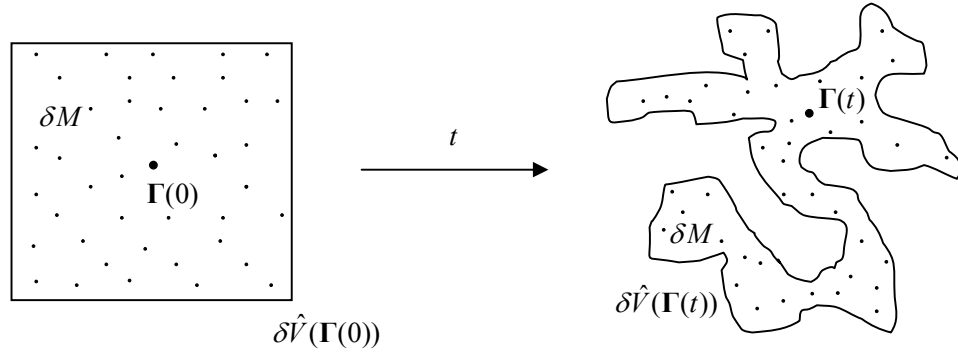


Figure 3.1. A schematic depiction of phase space compression, reproduced from (Cohen, 1994). The number of phase points δM does not change during deformation in time of the phase space volume element $\delta\hat{V}(\Gamma(0))$, centred on an initial condition $\Gamma(0)$.

Assuming the equivalence between ensemble and time averages, explicit formulae for $\langle \Lambda(\Gamma) \rangle$ in Eq. (3.15) will be derived and evaluated in Chapter 4 for different

thermodynamic constraints and used to test the accuracy of the computed Lyapunov exponent via (3.20). As an example of how phase space actually reduces for a nonequilibrium sample of particles, let us consider PSF SLLOD isokinetic thermostatted equations (1.32) and calculate (3.15). Omitting lower order terms in N due to the dependence of $\alpha(\Gamma)$ on Γ , we have

$$\langle \Lambda(\Gamma) \rangle_{\hat{V}(t)} = -3N \langle \alpha(\Gamma) \rangle_t \quad (3.21)$$

with the subscripts $\hat{V}(t)$ and t indicating an ensemble average and a time average at a steady state, respectively. Given that $\langle \alpha(\Gamma) \rangle_t > 0$, since heat is extracted from the system,

if we look at the last two expressions we conclude that $\sum_{i=1}^{6N} \lambda_i < 0$, so that the phase space shrinks when the system approaches the steady state. We notice that if CPR is satisfied, Eqs. (3.20)-(3.21) show that the contraction is applied “democratically” by the thermostat to all pairs of degrees of freedom.

The reduced subspace is an attractor for trajectories (Eckmann and Ruelle, 1985), has a fractal nature and its dimension D_{KY} can be calculated using the Kaplan-Yorke conjecture (Young, 1982; Frederickson *et al.*, 1983), which leads to the following formula in terms of the Lyapunov exponents:

$$D_{KY} = M + \frac{\sum_{i=1}^M \lambda_i}{|\lambda_{M+1}|} \quad (3.22)$$

where the exponents are ordered such that $\lambda_1 > \lambda_2 > \lambda_3 > \dots$ and M is the largest integer for which $\sum_{i=1}^M \lambda_i > 0$. Eq. (3.22) will be evaluated to compare phase space dimensions of PSF and PEF steady states at the same density and rate of energy dissipation, whereas the characteristics of attractors will be described in some generality in the next Section.

Finally, it is important to note that there exist an established link between transport coefficients and Lyapunov exponents in nonequilibrium systems (Posch and Hoover, 1988). This is realized by considering Gibbs’ definition of entropy

$$S = -k_B \int d\Gamma f(\Gamma, t) \ln f(\Gamma, t)$$

and taking its time derivative. Then, using the normalization property of $f(\Gamma, t)$ and two partial integrations, it is possible to relate the entropy production rate to the sum of the exponents using (3.17) and (3.20):

$$\dot{S} = -k_B \sum_{i=1}^{6N} \lambda_i \quad (3.23)$$

which gives an interpretation for the production of disorder in terms of the phase space contraction in the system. As we saw in Eq. (1.1), \dot{S} can also be expressed as a product of a thermodynamic flux and force, i.e. $\dot{S} = -V\mathbf{J}(\mathbf{F}_e) \cdot \mathbf{F}_e/T$, where V is the actual volume of the system. The dissipative flux $\mathbf{J}(\mathbf{F}_e)$ is given in terms of the adiabatic time derivative of the internal energy, or $\dot{H}_0 = -V\mathbf{J}(\mathbf{F}_e) \cdot \mathbf{F}_e$ (Evans and Morriss, 1990) and a transport coefficient $L(\mathbf{F}_e)$ is defined as $\mathbf{J}(\mathbf{F}_e) = -L(\mathbf{F}_e)\mathbf{F}_e$. For SLLOD PSF one finds

$$\dot{S} = -\frac{VP_{xy}\dot{\gamma}}{k_B T} \quad (3.24)$$

and, neglecting terms of order $O(1/N)$, an expression for shear viscosity under isokinetic or isoenergetic Gaussian constraints can be deduced⁵

$$\eta_{PSF} = -\frac{k_B \langle T \rangle}{\dot{\gamma}^2 V} \sum_{i=1}^{6N} \lambda_i \quad (3.25)$$

where brackets indicate the usual time average in the steady state. Equivalently, in case of isokinetic or isoenergetic SLLOD PEF samples, the following holds

$$\eta_{PEF} = -\frac{k_B \langle T \rangle}{4\dot{\epsilon}^2 V} \sum_{i=1}^{6N} \lambda_i \quad (3.26)$$

The importance of these results is twofold: firstly, if the system obeys CPR, we can replace the term for the sum of the exponents with just a single sum of our choosing, greatly simplifying the amount of computation required. For example, if we use the maximum and

minimum exponents, we can substitute $\sum_{i=1}^{6N} \lambda_i \rightarrow 3N(\lambda_{\max} + \lambda_{\min})$ into Eqs. (3.25)-(3.26)

and obtain results whose accuracy is comparable with that of direct NEMD time average

⁵ Temperature T is constant in isokinetic systems and its instantaneous value can be used in the calculations.

calculations. Secondly, and referring only to (3.25) for simplicity, we can rearrange the expression in the following way

$$\frac{\eta_{PSF}\dot{\gamma}^2V}{k_B\langle T \rangle} = -\sum_{i=1}^{6N} \lambda_i \quad (3.27)$$

and gain a simple insight into the connection between entropy production and phase space reduction. In fact, as the latter is given by the ratio of viscous heating $\eta_{PSF}\dot{\gamma}^2V$ with the intrinsic energy scale of the system $k_B\langle T \rangle$, this shows that irreversible processes that take place in the sample (such as collisions or friction) are responsible for the collapse of trajectories onto the lower dimensional attractor. For the interested reader, relations for transport coefficients of atomic thermostatted systems in terms of the Kaplan-Yorke dimension also exist (Evans *et al.*, 2000). Although we will repeatedly use expressions (3.25)-(3.26) in the next Chapter (appropriately modified for the case of two dimensional systems), it should be clear that the calculation of transport coefficients from Lyapunov exponents does not represent the most efficient and practical route. Despite the dramatic reduction in computational time that arises from the use of CPR, the lack of experimental means to measure the exponents and the fact that the algorithms for evaluating Eqs. (1.42)-(1.43) are simpler and generally faster, make NEMD time averages the most used method for the computation of viscosity and other transport properties.

We also stress that the connection between entropy production and phase space contraction does not belong to every nonequilibrium processes, as it is shown in the example of heat conduction in a random Lorentz gas (Lebowitz and Spohn, 1978; van Beijeren and Dorfman, 2000), a model that is introduced in the next Section.

3.3 Examples of chaos in nonequilibrium particle systems.

We now present a review of selected works regarding chaoticity in nonequilibrium systems, with particular attention towards those pertaining to the concepts just explained and using the methods of Nonequilibrium Molecular Dynamics (NEMD). We first introduce the Lorentz gas, discuss some of its properties especially when driven out of equilibrium, and briefly explain the connections with escape rate formalism and periodic orbit theory. Then, an exposition of major studies of chaos in many-particle atomic systems at equilibrium and under steady flows follows, with the aim of informing the reader with valid references for the next Chapter, where results for samples under PEF and PSF are detailed. We finally conclude with a presentation of two very active and debated topics: Lyapunov modes and fluctuation theorems.

3.3.1 The Lorentz gas.

Besides being the simplest nontrivial molecular dynamics model, the Lorentz gas possesses many interesting features that make it the subject of intensive studies from the point of view of statistical mechanics and chaotic dynamics. In its periodic version, it describes the motion of one or more point particles bouncing in an array of scatterers distributed in space according to some predetermined geometry, such as a hexagonal or square lattice (see Fig. 3.2). The interaction between the particles and the scatterers is usually regulated by a wall-like potential, making the collisions totally elastic with no recoil of the latter, thus mimicking the wandering of noninteracting electrons through a metallic crystal. If the shape of the rigid obstacles is assumed to be circular⁶ (or spheric in three dimensions), the one particle model can be shown to be an equivalent description of either two hard disks in a lattice with periodic boundary conditions, or of a so-called Sinai billiard, where boundaries are elastic and a single central scatterer is present. In these cases, it is also

⁶ The reader should be aware that different shapes lead to different diffusion properties (see Eq. (3.28)) and affect mixing and ergodicity. For instance, in two dimensions, circular scatterers in a hexagonal disposition lead to normal diffusion $\langle x^2 \rangle \sim t$, whereas triangular and square obstacles produce the trend $\langle x^2 \rangle \sim t \ln t$. In general, diverse forms of anomalous transport that depend, among other factors, on the geometry of the system can occur (see (Jepps and Rondoni, 2006) for a recent interesting review).

customary to replace the continuous time approach with the Poincaré section given by geometric considerations about collisions (see Fig. 3.2), interpreting the Lorentz gas as a discrete two dimensional chaotic map from a scatterer to the next. Its description is then completed with expressions for the time of flight and the displacement in the positions of the particle before and after a bounce.

It is not possible to give the reader a complete account of the many contributions that have been enriching the literature about this model, and we refer to (Dorfman, 1999; Bunimovich *et al.*, 2000) for a more detailed introduction. It is instead our objective to propose some of the views on the interrelation between chaoticity and statistical mechanics, with a focus on those results that employ NEMD procedures, thermostats and algorithms for nonequilibrium flows.

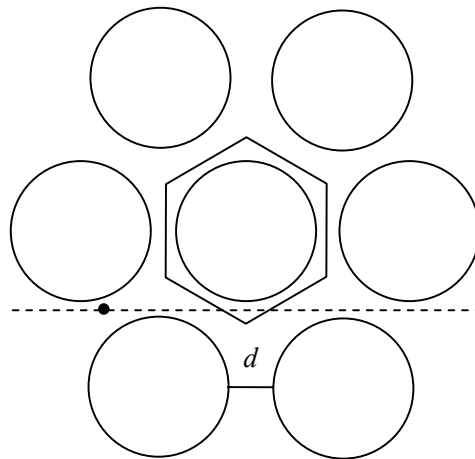


Figure 3.2. The periodic Lorentz gas with a hexagonal lattice of scatterers. For this arrangement, the case of infinite horizon is shown, meaning that the particle can escape from the array, as $d > 4/\sqrt{3} - 2$. A finite horizon, with an upper bound on time of flight, is instead given by $4/\sqrt{3} - 2 < d < 0$ and for $\sqrt{3} - 2 < d < 0$ scatterers overlap. The periodic cell is also depicted, pointing at the equivalence of the model with a hexagonal Sinai billiard when the horizon is finite. The radius of the scatterers is assumed to be unity.

The transport properties most commonly considered are diffusion and, in the presence of an external field, conductivity. In two dimensions and for one particle, the first property is defined as

$$D = \lim_{t \rightarrow \infty} \frac{\langle (\mathbf{x}(t) - \mathbf{x}_0)^2 \rangle}{4t} \quad (3.28)$$

where \mathbf{x}_0 is the initial position at time $t = 0$ and brackets indicate time averages. Following the analytical study of Bunimovich and Sinai in the limit of high density of circular disks (Bunimovich and Sinai, 1980), where a proof of the ergodicity of the model was provided, Machta and Zwanzig (Machta and Zwanzig, 1983) employed a random-walk approximation to establish a result for the diffusion coefficient in the low density regime (Klages and Dellago, 2000)

$$D_{MZ} = \frac{d(2+d)^2}{\pi [\sqrt{3}(2+d)^2 - 2\pi]} \quad (3.29)$$

where d is the distance between scatterers in a triangular arrangement and a rescaling of particle velocity v , mass m and radius of the obstacles r is made so that $v = r = m = 1$. If an external constant field $\mathbf{E} = E\mathbf{i}$ is driving the system along the x direction, the conductivity is given by

$$\kappa = \frac{\langle p_x(t) \rangle}{E} \quad (3.30)$$

$p_x(t)$ being the particle momentum in the x direction.

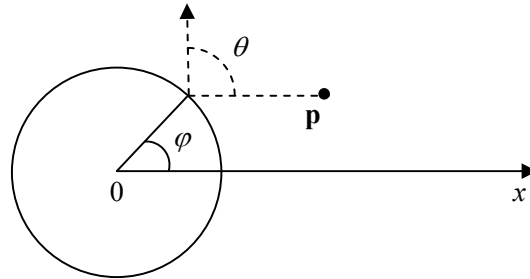


Figure 3.3. The continuous dynamics of the Lorentz gas is replaced by a discrete two-dimensional map in the variables θ and ϕ describing the change in the direction of momentum and the position of the particle on the surface of an obstacle during a collision.

NEMD has played an important role in the study of transport properties given by Eqs. (3.28)-(3.30) when external perturbations act on the system. For example, in (Moran *et al.*, 1987), investigations on conductivity have been realized for an isokinetic regime when a constant field \mathbf{E} is present, showing that κ is an overall decreasing function of E with

local minima and maxima that depend on the relative importance of first-, second- and third-neighbour collisions as the field strength changes. A planar shear flow (PSF) has been imposed with the use of DOLLS equations (1.8) coupled to a Gaussian thermostat in (Ladd and Hoover, 1984) and a shear-thinning behaviour for nonequilibrium viscosity analogous to that of N particle fluids seen in Section 2.3 has been found. An analysis of probability density, conductivity and distribution of periodic trajectories under different applications of Nosé–Hoover mechanisms for a constant field has also been performed recently in (Rateitschak *et al.*, 2000).

The chaotic properties of the Lorentz gas are particularly interesting and have been extensively detailed throughout the years. For instance, the calculation of Lyapunov spectra for nonequilibrium thermostatted steady states with the use of NEMD has been presented in the following works: (Dellago *et al.*, 1995), where a characterization of the phase-space fractal attractor in the case for a constant \mathbf{E} is given; (Baranyai *et al.*, 1992), where a test of CPR and an evaluation of diffusion and conductivity has been carried out; (Hoover and Moran, 1989), where the distribution of fractal domains in terms of the number of collisions at equilibrium and under a constant field have been analysed, and (Dettmann *et al.*, 1995), where the changes on the value of the exponents with the magnitude of the external field has been accurately studied, proving the independence of conjugate pairing from the ergodic properties of the system. Petravac and co-workers (Petravic, 1994; Petravac *et al.*, 1994) have produced an exhaustive discussion of the phase space distribution in the case of PSF SLLOD equations of motion, illustrating the properties of the fractal attractor and the time dependence in the synchronization of collisions. A formal justification of the validity of CPR at each instant t and for any number of particles N has been presented in (Dettmann and Morriss, 1996b) for the Gaussian isokinetic Lorentz gas and for equivalent hard sphere systems at equilibrium. This finding has been extended to NH dynamics in (Wojtkowski and Liverani, 1998) whereas a more accessible treatment can be found in (Panja, 2002). On the other hand, the case of a Gaussian ergostat with WCA scatterers has been discussed in (Bonetto *et al.*, 1998), showing that, although CPR does not hold at each instant for a single particle, numerical data suggest the validity of conjugate pairing at each t in the limit of large N . We also notice that an interesting proof of Lyapunov pairing using kinetic theory for a nonequilibrium, dilute, random Lorentz gas coupled to a Gaussian thermostat is given in (Latz *et al.*, 1997) and numerical simulations

for various densities are reported in (Dellago and Posch, 1997).

The Lorentz gas has also been instrumental in testing the connections between transport coefficients and Lyapunov exponents (Chernov *et al.*, 2005) and for a number of debates on fundamental issues such as those regarding, for instance, the role of chaoticity in diffusion processes (Dettmann and Cohen, 2000), the relationship between deterministic dynamics and the derivation of the laws of irreversible thermodynamics (Cohen and Rondoni, 2002), and the possibility of experimental detection of chaos in microscopic systems (Gaspard *et al.*, 1998; Dettmann *et al.*, 1999; Gaspard *et al.*, 1999).

In that sense, a clear example of an exact, analytical link between sensitivity to initial conditions and statistical mechanics for deterministic systems is contained in the celebrated work by Gaspard and Nicolis (Gaspard and Nicolis, 1990). This has constituted the basis of the so-called escape rate formalism, which is a general approach to relate chaotic dynamics and transport properties in deterministic systems (Gaspard and Dorfman, 1995; Gaspard, 1998). In the case of an infinite, regular triangular disposition of scatterers, the diffusion coefficient of the Lorentz gas can be shown to be

$$D = \lim_{R \rightarrow \infty} \left(\frac{R}{2.40482} \right)^2 [\lambda_{\max} - h_{KS}] \quad (3.31)$$

with R being the radius of a circumference centred in the middle of the array, and λ_{\max} and h_{KS} representing the maximum Lyapunov exponent and the Kolmogorov-Sinai entropy (Latora and Baranger, 1999), which, in systems with many degrees of freedom, can equivalently be expressed as the sum of all positive Lyapunov exponents (Pesin, 1977). The difference between the last two quantities in Eq. (3.31) denotes the escape rate γ : due to the defocusing character of collisions, in an initial collection of N_0 particles with identical velocity v and arbitrary initial positions, only a fraction $N(t) \sim N_0 e^{-\gamma t}$ remains in the vicinity of the disks, not going to infinity as t progresses.

The study of unstable periodic orbits in deterministic systems also represents a fundamental and elegant route to the evaluation of phase variables, dimensions of chaotic attractors and phase space distributions (Vance, 1992). This is achieved through an enumeration of cycles

and the construction of the so-called dynamical zeta function (Cvitanovic *et al.*, 2005). In fact, an observable A can be expressed as a weighted average of the contributions of periodic points:

$$\langle A \rangle = \lim_{\tau \rightarrow \infty} \frac{\sum_{i \in P_\tau} \Lambda_{1,i}^{-1} \cdot \int_0^{\tau_i} A(s) ds}{\sum_{i \in P_\tau} \Lambda_{1,i}^{-1} \cdot \tau_i} \quad (3.32)$$

where $\Lambda_{1,i}$ is the exponential of the sum of Lyapunov exponents multiplied by the period τ_i of cycle i , and P_τ is the set of unstable periodic orbits with periods close to τ . Loosely speaking, the idea that underpins this approach is that periodic orbits occur in a hierarchical, self-similar and tree-like structure, constituting the skeleton of chaotic dynamics and offering a way to express thermodynamical properties in terms of geometrical considerations on nonequilibrium trajectories. Examples of studies which apply this paradigm to the Lorentz gas can be found, among others, in the work by Cvitanovic *et al.* (Cvitanovic *et al.*, 1992), where diffusion is evaluated using a periodic orbit expansion, and in a series of papers (Lloyd *et al.*, 1994; Morriss and Rondoni, 1994; Lloyd *et al.*, 1995; Dettmann and Morriss, 1996c; Morriss *et al.*, 1996; Dettmann and Morriss, 1997b) where an extensive presentation on themes such as ergodicity, bifurcation diagrams, stability of trajectories and CPR at nonequilibrium is conducted with the use of cycles and the aid of numerical simulations.

3.3.2 Chaos in N -body liquids, Lyapunov modes and fluctuation theorems.

One of the first accurate studies of Lyapunov spectra for NH thermostatted atomic liquids is represented by (Posch and Hoover, 1988), where atoms are considered either in equilibrium or under a constant colour field F_e , which acts on particles tagged with fictitious opposite charges $c = \pm 1$. A functional dependence $\lambda(n) = \alpha n^\beta$ has been established for the positive branch of the spectrum at equilibrium, with $\lambda(n)$, α and β respectively being the n exponent and constants. Interestingly, β has a value close to $1/3$ similarly to the Debye model for the distribution of vibrational frequencies in solids, and this is also reflected in the good approximation of the maximum exponent to the Debye

frequency, which is proportional to the second derivative of the potential $\phi''(r)$ calculated at a separation R such that $\phi(R) = k_B T$. For $F_e \neq 0$, the loss in dimensionality due to the dissipative character of the steady state has been observed to be proportional to the square of the colour field and has later been proven to be extensive (Hoover and Posch, 1994). The authors have considered these facts as supportive of a resolution of Loschmidt's paradox in terms of the strange, lower dimensional nonequilibrium attractor (Holian *et al.*, 1987). In fact, in thermostatted systems that are described by reversible equations of motion, irreversibility seems to emerge from the inherent instability of second-law violating trajectories, which belong to the time-reversed, unstable and unobservable repellor (Hoover, 1999).

A further work focussed on dense two and three dimensional atomic systems, sampled with various boundary driven algorithms and basis cells, has analysed chaoticity at equilibrium and under shear flow with a NH isokinetic coupling (Posch and Hoover, 1989). Considerations on the convergence times for λ_{\max} , a complete representation of spectra at different system sizes and a comparison of NEMD chaotic features with continuum hydrodynamics constitute the main findings. This contribution has also suggested a functional form for the maximum exponent in terms of the number of atoms N . In (Searles *et al.*, 1997), a divergence of λ_{\max} with $\ln N$ for WCA particles at equilibrium has been observed numerically, regardless of the dimensionality of the system, whereas Hoover and Posch have computed λ_{\max} for increasing sizes of an atomic isoenergetic sample under SLLOD PSF in (Hoover and Posch, 1995). This study also contains observations on N dependence of nonequilibrium viscosity and a comparison of numerical results with Enskog's theory for dense fluids.

Sarman and co-workers (Sarman *et al.*, 1992), generalizing previous results by Morriss for smaller systems under shear (Morriss, 1989a), have provided a treatment of color field, thermal conductivity and SLLOD PSF algorithms, discussing the applicability of CPR to these models. Given the difficulty in applying the necessary conditions for conjugate pairing (3.10), limited accuracy in numerical calculations has induced the authors to conclude that equal sums occur in SLLOD PSF. Some years later, new computations have amended this observation (Searles *et al.*, 1998), showing deviations in instantaneous and

long time values of the Lyapunov sums for SLLOD PSF that do not scale with system size. On the other hand, Morriss has argued that the use of a block average procedure for the estimation of Lyapunov exponents has to be adopted to give better estimation of the error bars, which, with this method, are wider than the deviations from CPR for the Lyapunov sums of planar shear (Morriss, 2001). However, it should be noted that the simulation times in this study are much shorter than the ones in (Searles *et al.*, 1998), therefore the conclusions in the latter remain valid. Further, Morriss' results are in contradiction with the analytical treatment later presented in (Panja and van Zon, 2002b; 2002a), where, in the limit of small shear rate and large N , CPR is shown to be violated for isokinetic hard spheres under SLLOD dynamics at most at $O(\dot{\gamma}^4)$, because of the contribution of the $1/\sqrt{N}$ fluctuations in the Gaussian thermostat. We note that this debate has resulted from the very small departure from equal pairing, and, as said, numerical results for SLLOD PEF and PSF that are in line with a failure of CPR for the latter will be provided.

As explained, when a system satisfies equal pairing, the calculation of transport properties such as viscosity in terms of Lyapunov exponents is greatly simplified, and the knowledge of only a single sum in the spectrum is required. Once the highest exponent, which is also the fastest to converge, has been computed, it is possible to evolve the dynamics in negative time from the steady state used to calculate λ_{\max} and obtain λ_{\min} . Even when applied to SLLOD PSF, the procedure has given good estimates (Evans *et al.*, 1990), with an accuracy for nonequilibrium shear viscosity close to NEMD time averages. The lifetime and stability of backwards trajectories and their role in irreversibility has been carefully investigated in (Searles and Evans, 1996), whereas interesting observations regarding the consequences of Lyapunov instabilities for linear response theory have been put forward in (Morriss *et al.*, 1989). Connections among exponents, time correlation functions and Green-Kubo relations have been given in (Evans, 1992), finding that exponential separations of trajectories at short times are faster ($\sim e^{\lambda_{\max} t^2}$) than at long times ($\sim e^{\lambda_{\max} t}$) at equilibrium. Incidentally, Lyapunov spectra have also helped to establish some general properties of the Gaussian isokinetic thermostat (Evans and Baranyai, 1992; Sarman *et al.*, 1994; Bright *et al.*, 2005), since this is the only type which complies with CPR among the infinitely many constraints

that fix $\sum_{i=1}^N |\mathbf{p}_i|^{\mu+1}$, with $\mu=0,1,2\dots$. The case for $\mu=1$ shows other interesting extremum features, such as minimal phase space compression and maximal Kolmogorov-Sinai entropy.

As far as systems with hard core interactions are concerned, we note that an efficient algorithm for handling the collisions in hard disk systems when calculating Lyapunov exponents is detailed in (Dellago *et al.*, 1996). In this work, small and large collections of particles at equilibrium and under a colour perturbation have been discussed, with remarks about the dependence of spectra from density ρ , field strength and size of the sample. Numerical data on CPR are also present, and a proof of the well-known result by Krylov in the low density limit, $\lambda_{\max} \sim \rho \ln \rho$, is given (Krylov *et al.*, 1979).

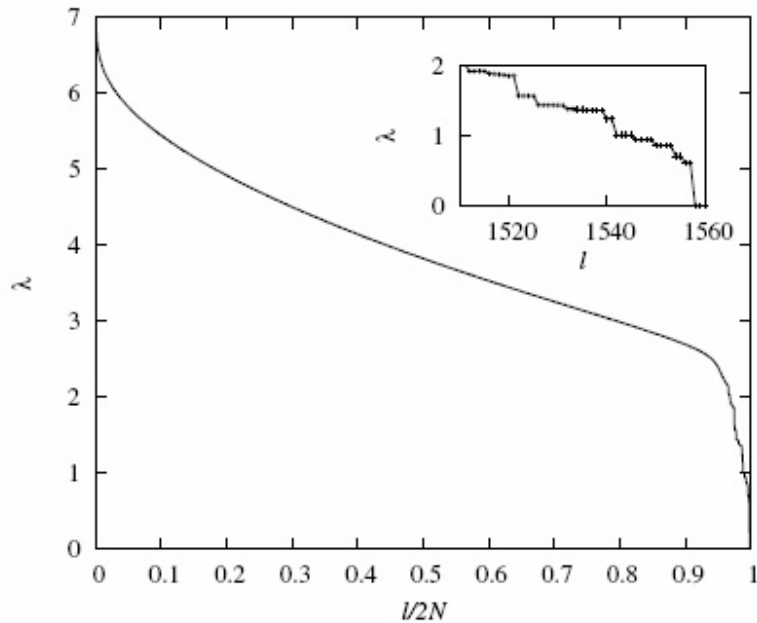


Figure 3.4. Lyapunov spectrum from (Eckmann *et al.*, 2005) for a system of $N = 780$ hard disks in a rectangular box with $L_y/L_x = 0.867$ and density $\rho = N/(L_x L_y) = 0.8$. The index l indicates the number of the exponent and the inset is a magnification of the eigenvalues associated to the Lyapunov modes.

With regards to recent developments in the field of chaotic dynamics, we note that a growing interest in the last few years has been devoted to the discovery and

characterization of the so-called Lyapunov modes, which are given by the eigendirections associated to the smallest exponents in the Lyapunov spectra of large N body systems. For systems at equilibrium, it has been found that the lowest positive (and negative) exponents display a high degeneracy and tend to appear in ladder-like structures, as indicated in Fig. 3.4.

This behaviour is a result of the collective contributions of almost all the particles to the slowly-growing (or decaying) perturbations in the system, and is associated with delocalized phenomena which can be linked to spread out fields in the tangent space. These can be identified by well-defined wave numbers k and have been interpreted as modes similar to the ones in hydrodynamics, with a simple expression of the harmonics in terms of the dimensions of the periodic (or reflecting) simulation box:

$$k = \sqrt{\left(\frac{2\pi}{L_x}n_x\right)^2 + \left(\frac{2\pi}{L_y}n_y\right)^2} \quad ; \quad n_x, n_y = 0, 1, \dots \quad (3.33)$$

where L_x and L_y are the boxlengths, and n_x and n_y count the number of nodes parallel to the x and y directions. Conversely, the value of the highest exponent is always dominated by the fastest growing (or decaying) and narrowly localized events in the sample, usually represented by two body collisions for hard disks, so that the number of particles contributing to λ_{\max} has been shown to tend to zero in the thermodynamic limit (Posch and Hoover, 2006).

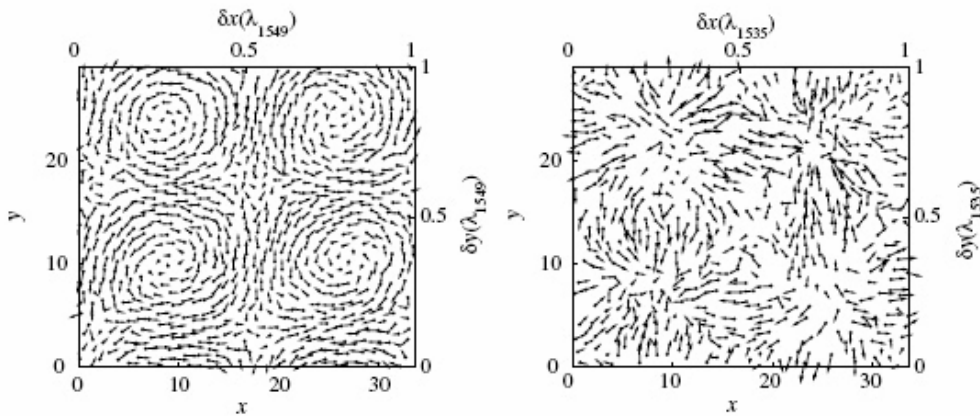


Figure 3.5. Lyapunov modes from (Eckmann *et al.*, 2005) for the same system in Fig. 3.4. Transverse modes associated to λ_{1549} are shown on the left, whereas irrotational fields belonging to λ_{1535} are on the right.

Lyapunov modes have been conjectured to arise from the so-called zero modes (for $k = 0$), which are associated to the null exponents in the spectrum and the conserved degrees of freedom in the system (see Subsection 4.2.2 for a comparison with the case of small N). As such, modes can be considered as representing the breaking of continuous symmetries in the model, and have been classified, for instance in the case of hard spheres, into two main groups depending on the type and degeneracy of the exponent they belong to (Eckmann *et al.*, 2005). There exist divergence-free translational modes and longitudinal ones, which are further subdivided into irrotational fields and scalar modulations of the momentum components of the Lyapunov eigenvectors (see Fig. 3.5).

A host of numerical and analytical data has been accumulating in the literature for various models at equilibrium, such as hard disks in various dimensions (Hoover *et al.*, 2002; Taniguchi and Morriss, 2003), one dimensional Lennard-Jones particles (Yang and Radons, 2005), WCA fluids⁷ (Forster and Posch, 2005), lattices of Hamiltonian and dissipative maps (Yang and Radons, 2006) and planar dumbbell liquids (Milanovic and Posch, 2002), also with suggestions about the existence of an experimentally accessible quantity for direct measurements (Taniguchi and Morriss, 2005). Lyapunov exponents and their associated modes have been calculated with several different approaches, among which random matrix theory (Eckmann and Gat, 2000; Taniguchi and Morriss, 2002), kinetic theory (McNamara and Mareschal, 2001; Mareschal and McNamara, 2004) and periodic orbit expansions (Taniguchi *et al.*, 2002) have been the most effective.

Another very active field of research in the context of nonequilibrium liquids which is tightly interwoven with chaotic dynamics is represented by the so-called fluctuation theorems. The idea of expressing transport coefficients with the use of thermal or mechanical oscillations in the system draws back to the fundamental works of Boltzmann, Einstein, Smoluchowski, Onsager and many others. Nonetheless, it has recently been possible to derive an extension of the second law of thermodynamics for out of equilibrium samples and give an exact account for the probability of observing phase space trajectories

⁷ The identification of modes for systems interacting via soft potentials appears to be more involved than the case of hard core interactions and presents some technical difficulties that have been recently overcome with the use of Fourier transforms. This led some authors to be initially sceptical about the existence of Lyapunov modes for soft systems (Forster *et al.*, 2004).

associated to a negative variation in the entropy of the system. In 1993, Evans and co-workers (Evans *et al.*, 1993) postulated that positive Lyapunov exponents can be used to define a natural invariant measure for trajectory segments of an N body system in a steady state:

$$\mu_i(\tau) = \frac{\exp\left[-\sum_n \lambda_{i,n} \tau\right]}{\sum_i \exp\left[-\sum_n \lambda_{i,n} \tau\right]} \quad (3.34)$$

where $i = 1, \dots, M$ indicates those segments on each of which the sample spends a time τ and the relation holds in the limit of sufficiently large τ . With this hypothesis, an expression for the average density of entropy production σ for a steady state can be found

$$\frac{P(\langle \sigma \rangle_\tau = A)}{P(\langle \sigma \rangle_\tau = -A)} = e^{A\tau} \quad (3.35)$$

$P(\langle \sigma \rangle_\tau = A)$ indicates the probability of having an average value of σ in the interval $[A, A + dA]$ for a length of averaging time τ . Formula (3.35) represents the so-called steady state fluctuation theorem, and shows that the likelihood that entropy flows in a direction opposite to the second law of thermodynamics with a value $-A$ decreases with τ , the magnitude of σ and the degrees of freedom in the system, and does not directly depend on the strength of the external field. Similar expressions for other observables can be obtained and an illustration of the probability distribution of shear stress for isoenergetic SLLOD PSF is given by Fig. 3.6. In this case, since $\langle P_{xy} \rangle$ is proportional to the negative of time-averaged entropy production for Eq. (3.24), Eq. (3.35) assumes an equivalent form

$$\frac{P(\langle P_{xy} \rangle_\tau = A)}{P(\langle P_{xy} \rangle_\tau = -A)} = \exp\left[-\frac{AV\dot{\gamma}\tau}{k_B T}\right] \quad (3.36)$$

This type of relation has later been derived in a rigorous way using Lyapunov weights (Jepps *et al.*, 2004), arriving at the so-called transient time Evans-Searles fluctuation theorems, which possess a more general applicability (Evans and Searles, 2002). Among their properties, these relations are exact for arbitrary averaging times, apply to a variety of thermodynamic constraints and are appropriate for far from equilibrium regimes. A steady state version can also be obtained, which leads to the Green-Kubo relations for the transport

coefficients in the linear regime (Evans *et al.*, 2005). In general, the transient relations only suppose the reversibility of microscopic dynamics and concern the statistics of a dissipation function Ω for an ensemble of systems evolving out of equilibrium, with no restrictions on τ :

$$\frac{P(\langle \Omega \rangle_\tau = A)}{P(\langle \Omega \rangle_\tau = -A)} = e^{A\tau} \quad (3.37)$$

where, for NEMD, Ω has the physical meaning of a generalized entropy production rate. With the use of optical trapping experiments (Wang *et al.*, 2002; Carberry *et al.*, 2004; Wang *et al.*, 2005), laboratory confirmations for Evans-Searles fluctuation theorems have been established and their validity has been proven also for stochastic systems (Searles and Evans, 1999).

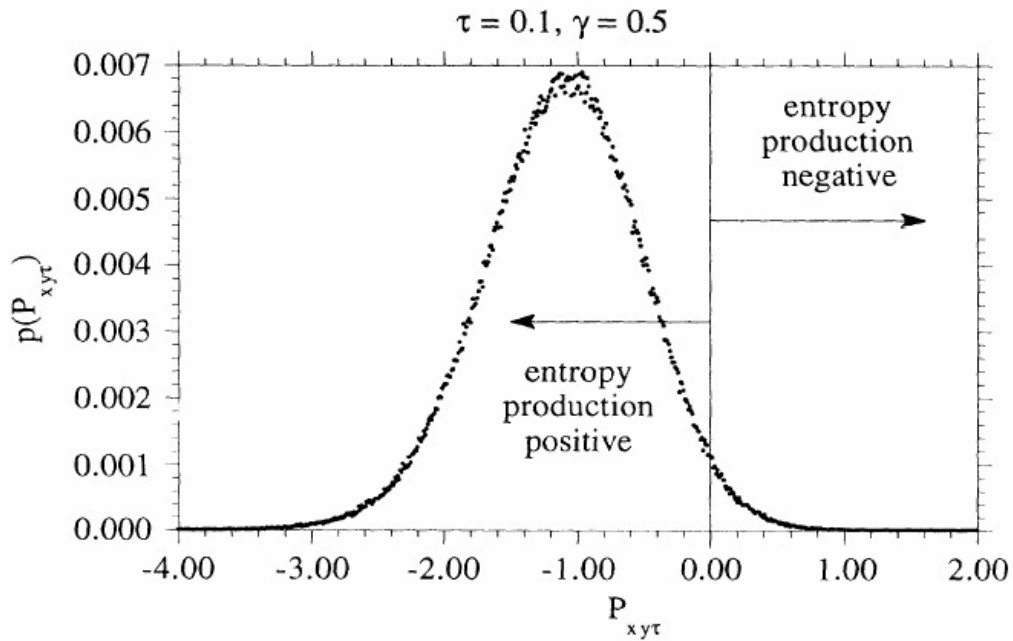


Fig. 3.6. Probability distribution for the average of the shear stress for 56 isoenergetic WCA disks with density $\rho = 0.8$, shear rate $\dot{\gamma} = 0.5$, and length of averaging time $\tau = 0.1$. States with a positive value of $\langle P_{xy} \rangle$ are responsible for a negative entropy production for a period of time τ , contrary to the second law of thermodynamics. The curve is approximately Gaussian. Reproduced from (Evans *et al.*, 1993).

It should be noticed that other important and analogous fluctuation relations have been proposed throughout the years, among which the most relevant are Crook's generalized

equation for work differences (Crooks, 1999), Jarzynski's equivalence for free energies (Jarzynski, 1997) and Gallavotti-Cohen's theorem for the phase space contraction in systems satisfying the so-called "chaotic hypothesis" (Gallavotti and Cohen, 1995). All these expressions have a great relevance for small systems such as those of interest for nanotechnology and biology, where the probability of detecting negative entropy production increases exponentially with the reduction of spatial and time scales in observation (Bustamante *et al.*, 2005).